Article

Analysis of the Fuel Properties of the Seed Shell of the Neem Plant (*Azadirachta indica*)

Francisco Simão Neto [1], Maria Melo Neta [2], Ana Sousa [1], Luana Damasceno [2], Bruna Sousa [2], Samuel Medeiros [3], Rafael Melo [4], Ada Lopes [5], José Santos [5] and Maria Rios [1,2,*]

1   Departamento de Engenharia Química, Universidade Federal do Ceará, Fortaleza 60440-900, Brazil;
    fcosimao@aluno.unilab.edu.br (F.S.N.); anasales@alu.ufc.br (A.S.)
2   Departamento de Engenharia Mecânica, Universidade Federal do Ceará, Fortaleza 60440-900, Brazil;
    marliete@alu.ufc.br (M.M.N.); luanabd@alu.ufc.br (L.D.); araujobrsousa@gmail.com (B.S.)
3   Departamento de Engenharia Metalúrgica e de Materiais, Laboratório de Materiais Avançados,
    Universidade Federal do Ceará, Fortaleza 60440-900, Brazil; samuel_engmat@ufc.br
4   Curso Técnico em Manutenção Automotiva, Campus Tabuleiro do Norte, Instituto Federal do Ceará,
    Tabuleiro do Norte 62960-000, Brazil; rafael.melo@ifce.edu.br
5   Instituto de Engenharias e Desenvolvimento Sustentável, Universidade Integração Internacional da Lusofonia
    Afro-Brasileira, Redenção 62790-000, Brazil; ada@unilab.edu.br (A.L.); jcs@unilab.edu.br (J.S.)
*   Correspondence: alexsandrarios@ufc.br; Tel.: +55-85-999831492

Abstract: The energetic potential of the seed shell of the Neem plant (*Azadirachta indica*) was investigated using proximate analysis, Higher Heating Value (HHV), thermal analysis (TG-DTG and DSC) in inert and oxidative atmospheres, and X-ray fluorescence (XRF). The results of ash (3.80% ± 0.44), volatile matter (81.76% ± 1.30), fixed carbon (14.44% ± 1.74), and estimated HHV (18.791 MJ/kg: average value) are compatible with other biomasses already used as fuels in the bioenergy industry. Thermograms showed three main degradation events in synthetic air and two in nitrogen, attributed to the moisture, release of volatile materials, and decomposition of hemicellulose, cellulose, and lignin. The elements positively detected by the XRF were Ca, K, S, P, Fe, Ti, Zn, Rb, and Sr.

Keywords: Neem; proximate analysis; bioenergy; alternative source; plant biomass; TG; XRF

1. Introduction

It is incontestable that society is increasingly dependent on energy [1]. Thus, alternative sources are necessary to address the growing demand for new technologies that need a significant amount of energy to be developed [2–4]. Alternatives to energy demand are biofuels that present a reduction in greenhouse gases, possess less pollution in their production line, possibility the integrated use, and characteristics compatible with conventional fuels [5–11].

Among possible feedstocks for biofuel production is the Neem tree (*Azadirachta indica*), which already has some applications in the bioenergy sector, such as charcoal (trunk), briquettes (leaves and stem bark), and biodiesel (oil extracted from seeds) [12–16]. Neem is a plant native to India and the adjacent regions, which has adapted to the climate of northeastern Brazil, allowing local production and a possible application as feedstock for biofuel production [17,18]. Several researchers have also studied the Neem tree, evaluating its medicinal, antiseptic, and insecticide properties [19]. In addition, the oil extracted from the seed has been used in personal care items, insect repellent, and pesticides [20–22].

Some studies show that Neem seed kernel contains about 45% of oil [19], composed of oleic acid (50–60%), palmitic acid (13–15%), stearic acid (14–19%), linoleic acid (8–16%), and arachidic acid (1–3%), showing potential for the production of biodiesel and biolubricants. Furthermore, many chemicals have been identified from the seeds [23], and Saleem et al. (2018) [24] reported the presence of other beneficial compounds in the whole Neem tree, including its flowers, bark, twigs, gum, sap, and leaves. For example, Neem

leaf and seed formulations exhibit antibacterial properties, antifeedant activities, roles in lowering fecundity, ovicidal and larvicidal activities, growth inhibition properties, and repellence activities against insect vectors [22,25].

After Neem seed oil extraction, a cake is formed [26], and an extract also can be obtained when the cake is extracted with solvent [27]. These byproducts can be further processed, crystallized, emulsified, and mixed with solvents for use in processes based on Neem compounds [28–30]. Regarding Neem leaves, Rao and Murugan (2023) [31] report that their natural extracts have been used in cosmetic formulations, insect-repellent soaps, and lubricant production. Moreover, they have proven therapeutic properties and healing benefits, being considered a traditional remedy to treat several health problems [32]. Thus, the Neem tree is recognized by the National Academy of Science, USA as '*A tree for solving global problems*' [33].

For energetic applications, some authors have used parts of the Neem tree, such as leaf waste, as feedstock for gasification [34]. Kumar et al. (2021) [34] evaluated the energetic potential of Neem leaf waste using proximate and elemental analyses and Higher Heating Value. The results showed better than rice husk and coal, indicating that it can be applied as biofuel for cooking and in small-scale industries. Due to its low sulfur concentration, Neem leaf waste has the potential to satisfy human needs without harming the environment, ensuring energy security and sustainability. However, the energetic potential of the seed shell of the Neem plant has not been explored. Thus, aiming for the integrated harnessing of the tree and contributing to the area of renewable energy, the authors developed this work.

In the solid fuel class is the briquette, a prominent alternative to energy generation [35,36]. Briquettes can be produced from residual biomasses or mixed with them and used to generate thermal energy in furnaces and boilers [37,38]. The property of each biomass contributes to the quality of the mixture and is based on moisture content, total solids, ash, volatile matter, and fixed carbon [39,40].

Moisture, volatile matter, ash, and fixed carbon contents compose the proximate analysis, which is essential to the biofuel evaluation [41]. Furthermore, total solids can be determined and assist in the indication of better mixing of biomasses for briquettes production [42].

Thermal analysis is one of the techniques most used to investigate the thermal behavior of lignocellulosic biomass [43–46]. In thermogravimetry (TG), data are collected by the progress of mass change versus temperature, and the thermogram can be used to obtain the volatile matter and ash quantities as well as the differences in thermal response due to varying proportion of the hemicellulose, cellulose, and lignin [47]. Differential scanning calorimetry (DSC) allows one to measure the thermal properties of biomass by establishing the between temperature and physical properties and determining the enthalpy associated with the process of interest [48].

The inorganic elemental analysis of biomass is essential for increasing its utilization as biofuel, and X-ray fluorescence (XRF) spectrometry is an attractive method for this evaluation. Morgan et al. 2015 [49] inferred that the XRF method could be used to estimate the ash yield from biomass combustion and considered for general use in industrial laboratories. Biomass characterization through XRF allows the detection of ash-forming compounds and corrosive elements that can deteriorate the equipment used in thermal conversion processes [50].

Thus, the work shows the analysis of the energetic potential of the seed shell of the Neem plant (*Azadirachta indica*) as potential biomass for the future production of briquettes. For this, moisture, volatile matter, ash, fixed carbon, and total solid contents were determined, and the results were compared with other biomasses published in the literature. In addition, the thermal behavior of biomass was analyzed by TG-DTG and DSC using nonisothermal conditions in synthetic air and nitrogen atmospheres, and the inorganic elemental analysis by X-ray fluorescence (XRF).

2. Materials and Methods

2.1. Materials

The fruits were collected in January 2021, Fortaleza-CE-Brazil, geographical coordinates—Latitude: 2°31′51″ S and Longitude: 44°18′24″ W. Figure 1 shows the steps for the preparation of the Neem seeds.
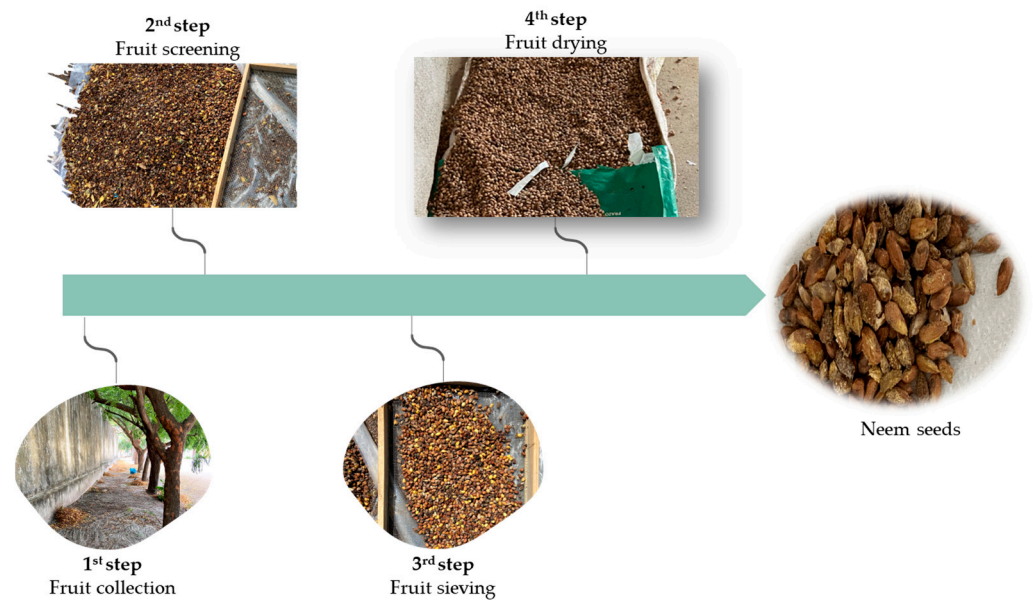

Figure 1. Steps for the preparation of the Neem seeds.

After collection, Neem fruits were screened (2nd step) for branches, leaves, and separation of other impurities. In sequence, the sieve operation removed sand and other dirt (3rd step), and then fruits were stored in plastic bags and taken to the drying stage (4th step), in which they were exposed to the sun for 60 days. Cores and shells were obtained from dried fruits (Figure 2).

Figure 2. Neem seed: core and shell.

The separation of the shell and core was carried out using a large sieve. To facilitate the process, it was necessary to hydrate the seeds to obtain the core and a fibrous mass (Figure 3). Subsequently, the materials were subjected to sun-drying again.

Figure 3. Fibrous mass and core from Neem seeds.

2.2. Proximate Analysis

Moisture and total solid contents were determined following NBR 16550 (Equations (1) and (2)) [51]

$$Moisture\ (\%) = \left(\frac{m_{Si} - m_{Sf}}{m_{Si}}\right) \times 100 \tag{1}$$

$$Total\ Solids\ (\%) = \left(\frac{m_{Sf}}{m_{Si}}\right) \times 100 \tag{2}$$

where: m_{Si} = mass sample as received (g) and m_{Sf} = mass dry sample (g).

For the procedure, we used 1.0 g of sample and a drying oven at temperature of $105 \pm 3\ °C$ for 2 h. The experiment was repeated until mass was constant.

For analysis of ash content, we used approximately 1.0 g of the sample and a muffle furnace at a temperature of $575 \pm 25\ °C$ for 4 h (Figure 4). The content was calculated using Equation (3) (NBR 16550 [51]).

$$Ash\ (\%) = \left(\frac{m_{Ash}}{m_{Sf}}\right) \cdot 100 = \left(\frac{m_{Ash} \cdot 100}{m_{Si} \cdot TS(\%)}\right) \cdot 100 \tag{3}$$

where: m_{Ash} = mass of total ash (g); m_{Sf} = mass dry sample (g); m_{Si} = mass sample as received (g); and $TS(\%)$ = total solid percentage.

Figure 4. Shell samples for analysis: (**a**) ceramic crucibles after volatile matter content determination and (**b**) ceramic crucibles after ash content determination.

Volatile matter content was determined following ASTM D3175-20 [52], using approximately 1.0 g of dry sample and a muffle furnace at 950 °C for 7 min; see Figure 4. The content was calculated by Equation (4).

$$Volatile\ Matter\ (\%) = \left[\left(\frac{m_i - m_f}{m_f - m_{c+l}}\right) \cdot 100\right] - M(\%) \tag{4}$$

where: m_i = initial mass of porcelain crucible with lid plus sample (g); m_{Sf} = final mass of porcelain crucible with lid plus sample (g); m_{c+l} = mass of porcelain crucible with lid (g); and $M(\%)$ = moisture percentage.

The fixed carbon content was calculated by Equation (5), following the methodology proposed in ASTM D3172-13(2021)e1 [53].

$$Fixed\ Carbon\ (\%) = 100 - Ash(\%) - Volatile\ Matter(\%) \tag{5}$$

The Higher Heating Value was estimated using the proximate analysis results (Equations (6)–(12)) [54–59].

$$HHV\left(\frac{MJ}{kg}\right) = 0.3536 \cdot Fixed\ carbon(\%) + 0.1559 \cdot Volatile\ Matter(\%) - 0.0078 \cdot Ash(\%) \tag{6}$$

$$HHV\left(\frac{MJ}{kg}\right) = -17.507 + 0.3985 \cdot Volatile\ Matter(\%) + 0.2875 \cdot Fixed\ carbon(\%) \tag{7}$$

$$HHV\left(\frac{MJ}{kg}\right) = -2.057 - 0.092 \cdot Ash(\%) + 0.279 \cdot Volatile\ Matter(\%) \tag{8}$$

$$HHV\left(\frac{MJ}{kg}\right) = 0.1905 \cdot Volatile\ Matter(\%) + 0.2521 \cdot Fixed\ carbon(\%) \tag{9}$$

$$HHV\left(\frac{MJ}{kg}\right) = 0.196 \cdot Fixed\ carbon(\%) + 14.119 \tag{10}$$

$$HHV\left(\frac{MJ}{kg}\right) = 157.34 \cdot (Volatile\ Matter(\%) + Fixed\ carbon(\%)) + 4243.97 \tag{11}$$

$$\begin{aligned} HHV\left(\frac{MJ}{kg}\right) &= 0.365 \cdot Fixed\ carbon(\%) + 0.131 \cdot Volatile\ Matter(\%) + \left(\frac{1.397}{Fixed\ carbon(\%)}\right) \\ &+ \left(\frac{328.568 \cdot Volatile\ Matter(\%)}{10283.138 + 0.531 \cdot (Fixed\ carbon(\%))^3 \cdot Ash(\%) - 6.863 \cdot (Fixed\ carbon(\%))^2 \cdot Ash(\%)}\right) \end{aligned} \tag{12}$$

where: HHV = Higher Heating Value $\left(\frac{MJ}{kg}\right)$.

2.3. Thermal Analysis

The thermal analyses were performed in a NETZSCH STA 449 F3 Jupiter®–Thermal Analysis System. The parameters were: sample mass of 20 mg, temperature range of 25–800 °C, nitrogen, and synthetic air (20% oxygen and 80% nitrogen) atmospheres with a flow rate of 50 mL min^{-1} and heating rate of 10 °C min^{-1}. The plots of mass loss versus temperature and flux heat versus temperature were generated using the NETZSCH Proteus® software (version 5.2.0).

2.4. X-ray Fluorescence (XRF)

The energy-dispersive X-ray fluorescence (XRF) spectrometer was the EDX 7000 equipped with a rhodium tube from Shimadzu Corporation (Japan), operating with the PCEDX Navi software from Shimadzu (https://www.shimadzu.com/an/sites/shimadzu.com.an/files/

The conditions were excitation of 20 kV, 100 μA, a collimator of 10 mm, atmosphere of He, a filter of Al (25 μm thickness), the integration time of 800 s, chlorine line Ka of 2.62 KeV, energy peak integration range of 2.55–2.82 KeV. A 31 mm (diameter) polyethylene cell, sealed with a polypropylene film (5 μm thickness), was used to hold the sample. The X-ray beam focused on the bottom window of the cell. The biomass sample (about 100 mg) was directly introduced in the polyethylene cell without previous preparation and placed into the automatic sampling carrousel. Background (BG) correction was made by measuring the integrated intensity of the range over the auto-BG line.

3. Results

The results of the proximate analysis of the Neem seed shell and other biomasses from the literature for comparison [60–64] are shown in Table 1.

Table 1. Proximate analysis of the Neem seed shell and other biomasses from the literature.

Biomass	Moisture (%)	Ash (%)	VM (%)	FC (%)	References
Neem seed shell	12.68 ± 0.16	3.80 ± 0.44	81.76 ± 1.30	14.44 ± 1.74	This work
Neem leaves	10.4	7.41	92.59	24.82	[60]
Neem wood	7.33	0.46	82.29	17.25	[61]
Coconut shell	7.32	1.42	69.21	30.09	[62]
Sugarcane bagasse	7.94	2.15	82.72	15.12	[63]
Eucalyptus wood	9.03	0.54	86.73	12.73	[64]

VM = volatile matter, FC = fixed carbon.

Figure 5 shows the results of the proximate analysis of the Neem seed shell.
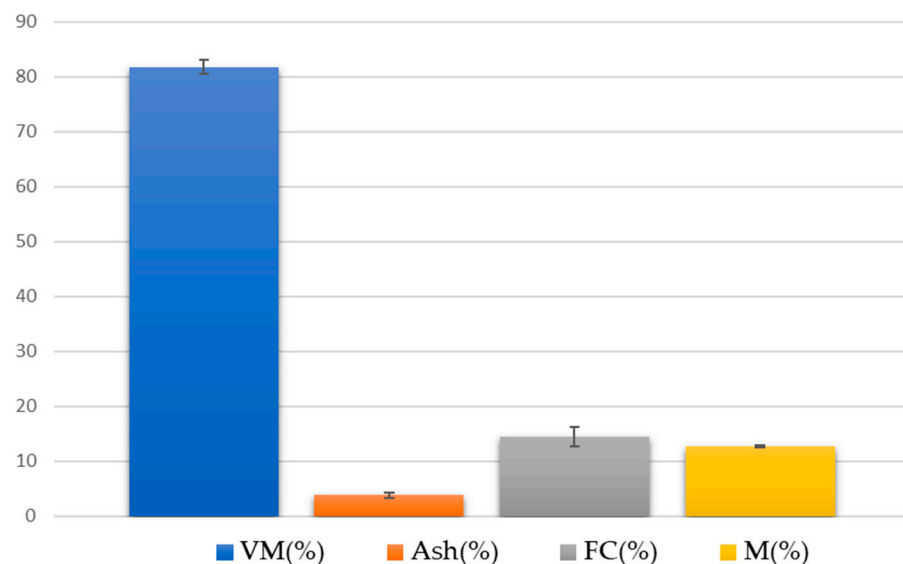

Figure 5. Volatile matter content (VM%), ash content (Ash%), fixed carbon content (FC%), and moisture content (M%) of the Neem seed shell.

Figure 6 presents the results of the seed shell, leaves, and wood of the Neem. The results of the leaves and wood are from the literature [65–67].
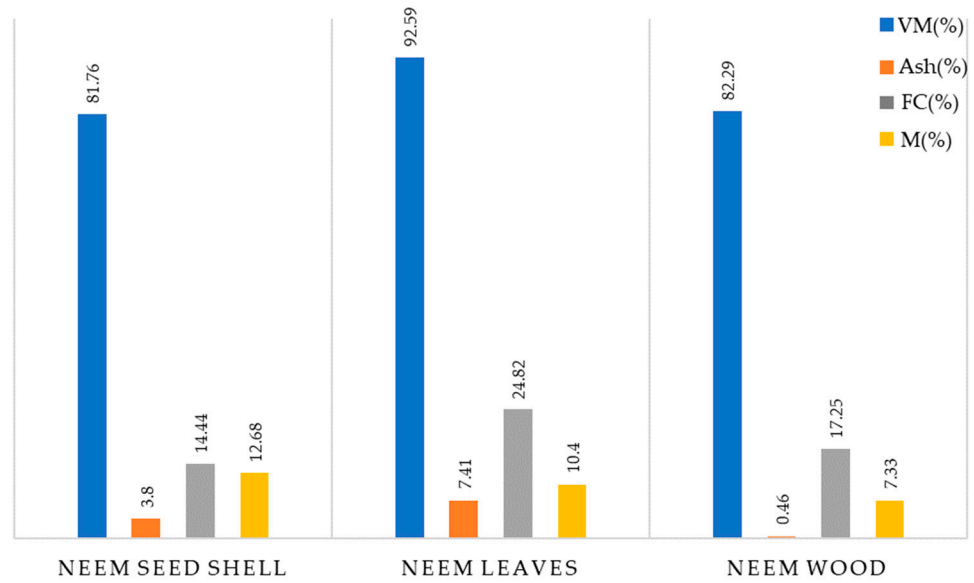
Figure 6. Volatile matter content (VM%), ash content (Ash%), fixed carbon content (FC%), and moisture content (M%) of the seed shell, leaves, and wood of the Neem [65–67].

Figure 7 shows the estimated results of the Higher Heating Value (HHV, MJ/kg) of the seed shell, leaves, and wood of the Neem, based on Equations (6)–(12) [54–59] presented in the Materials and Methods section.
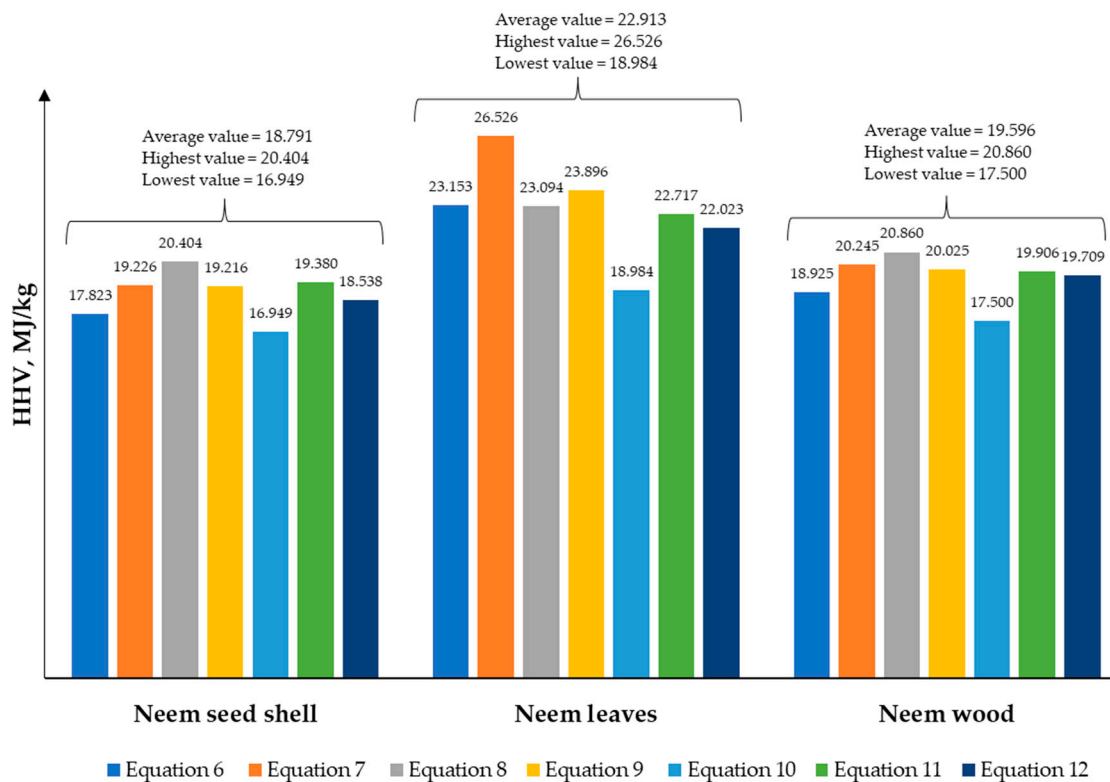

Figure 7. Higher heating value (MJ/kg) estimated by Equations (6)–(12) [54–59] for seed shell, leaves, and wood of the Neem.

Table 2 presents the average values of the Higher Heating Value (HHV, MJ/kg) estimated by Equations (6)–(12) [54–59] for the biomasses coconut shell [62], sugarcane bagasse [63], and eucalyptus wood [64].

Table 2. Average values of the Higher Heating Value (HHV, MJ/kg) estimated by Equations (6)–(12) [54–59] for the biomasses coconut shell [62], sugarcane bagasse [63], and eucalyptus wood [64].

Biomass	HHV, MJ/kg
Coconut shell	19.864
Sugarcane bagasse	19.156
Eucalyptus wood	19.422

The results of the thermogravimetric (TG-DTG) and DSC curves of the seed shell of the Neem plant (*Azadirachta indica*) are presented in Figures 8–10.
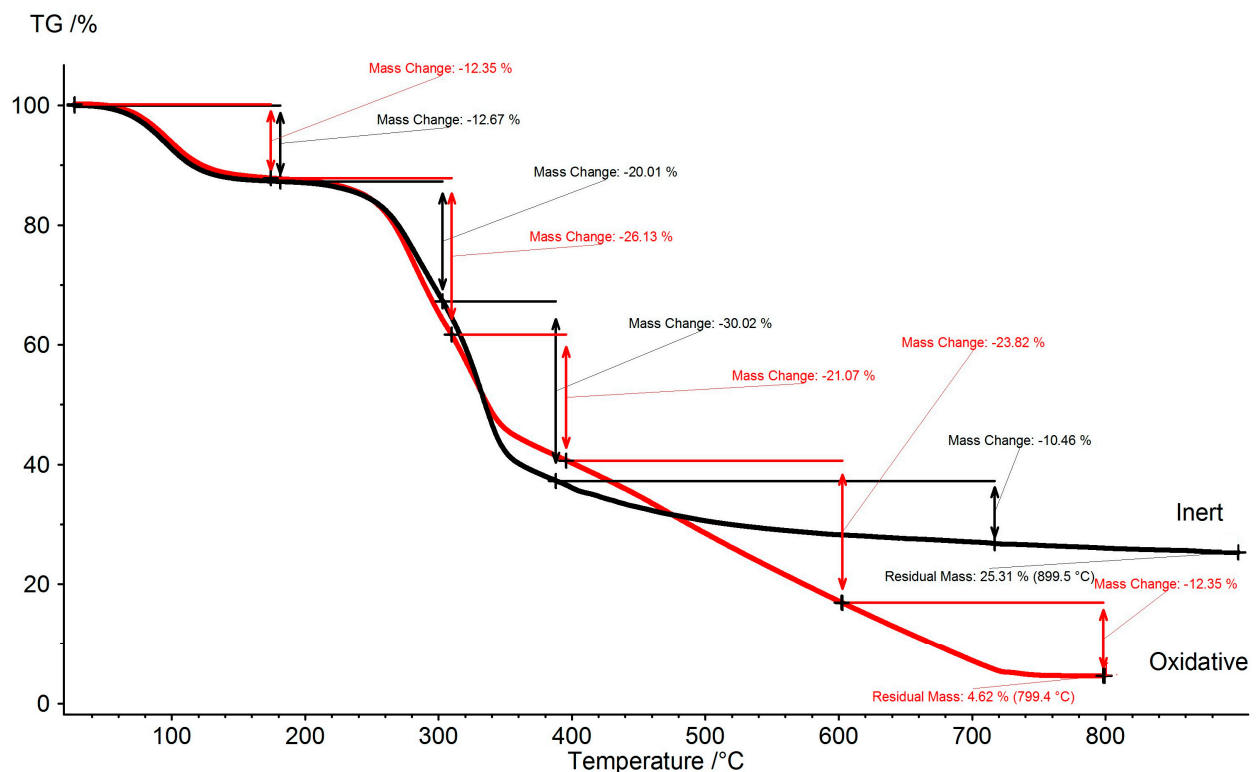

Figure 8. TG curves of the seed shell of the Neem plant, at 10 °C min^{-1} heating rate: red line synthetic air atmosphere and black line nitrogen atmosphere.

Tables 3 and 4 present the results of the thermogravimetry (TG-DTG) and differential scanning calorimetry (DSC) of the Neem seed shell in atmospheres of synthetic air and nitrogen.

Table 3. Results of TG-DTG of the Neem seed shell in the atmosphere of synthetic air and nitrogen.

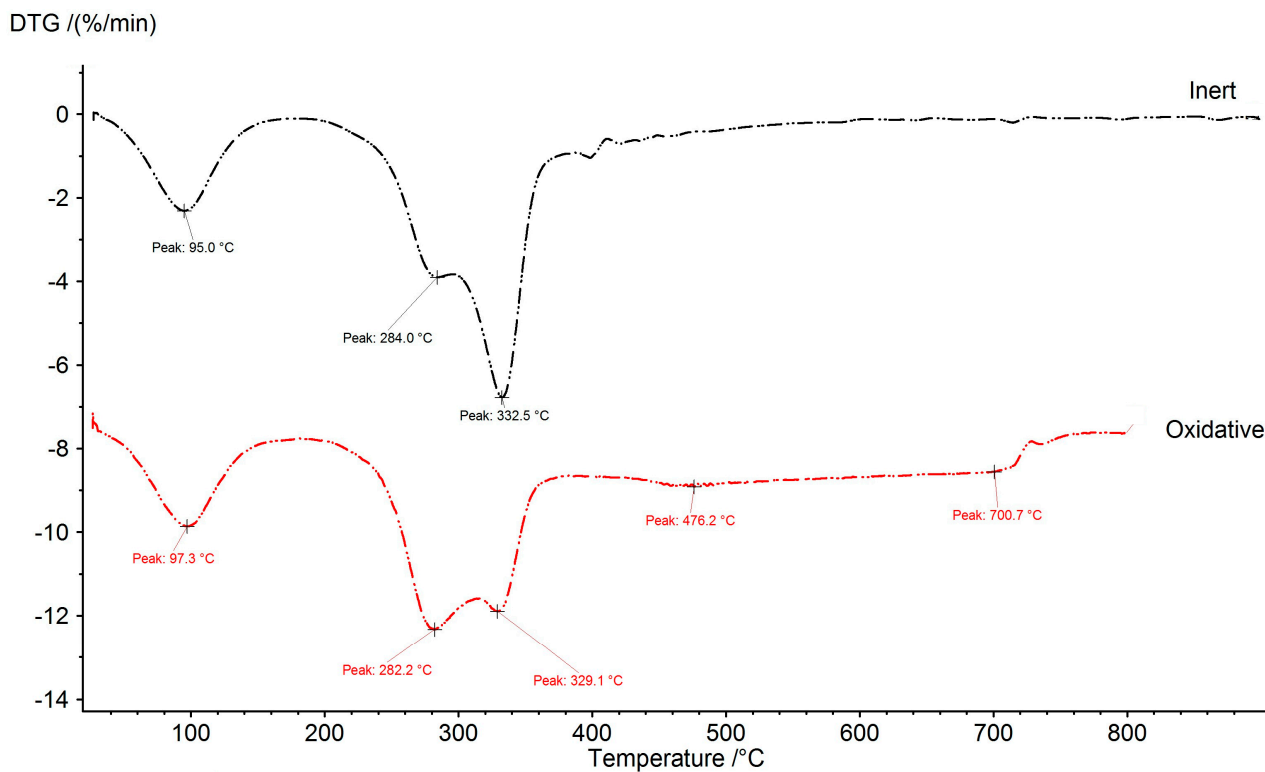| Synthetic Air				
Event	T_{onset}/°C	T_{peak}/°C	T_{endset}/°C	Mass Change %
1	57.8	97.3	135.2	12.35
2	243.2	282.2	357.3	47.20
3	414.3	329.1	733.6	36.17
Nitrogen				
Event	T_{onset}/°C	T_{peak}/°C	T_{endset}/°C	Mass Change %
1	54.9	95.0	137.2	12.67
2	241.8	332.5	355.1	50.03

Figure 9. DTG curves of the seed shell of the Neem plant, at 10 °C min^{-1} heating rate: red line synthetic air atmosphere and black line nitrogen atmosphere.
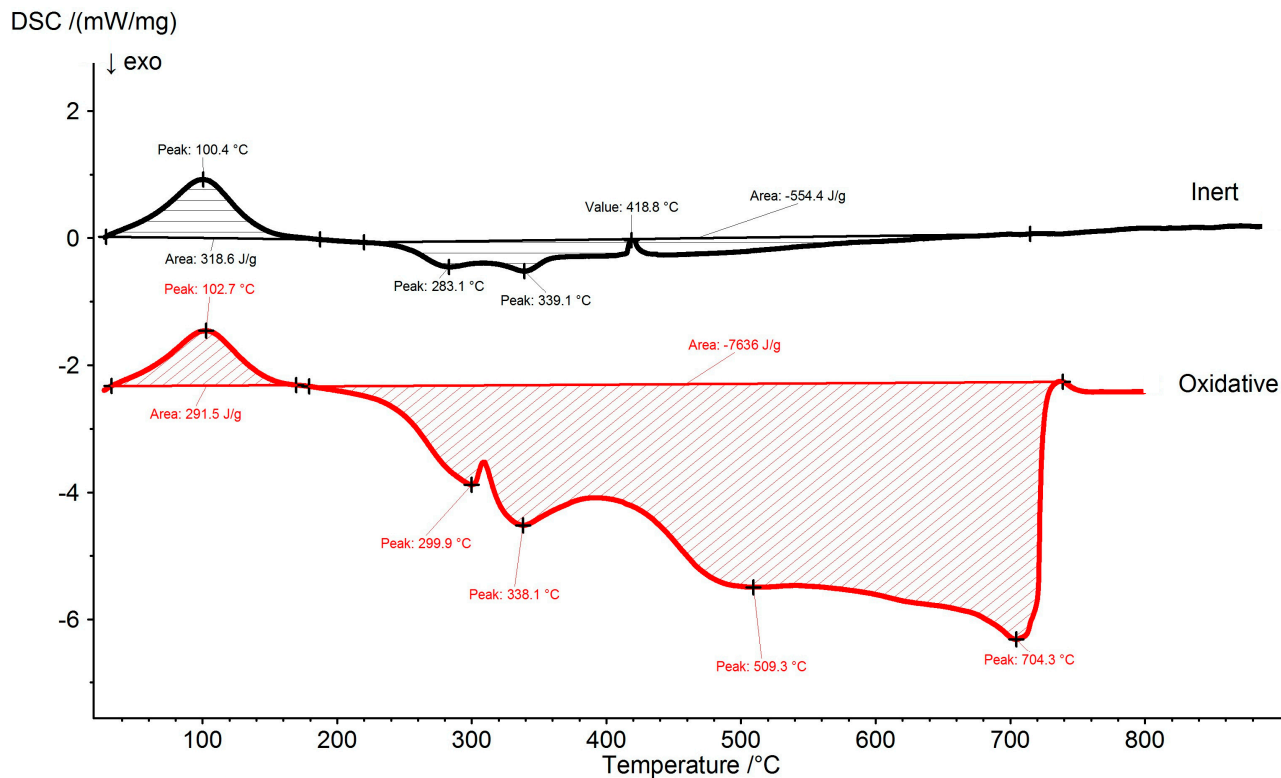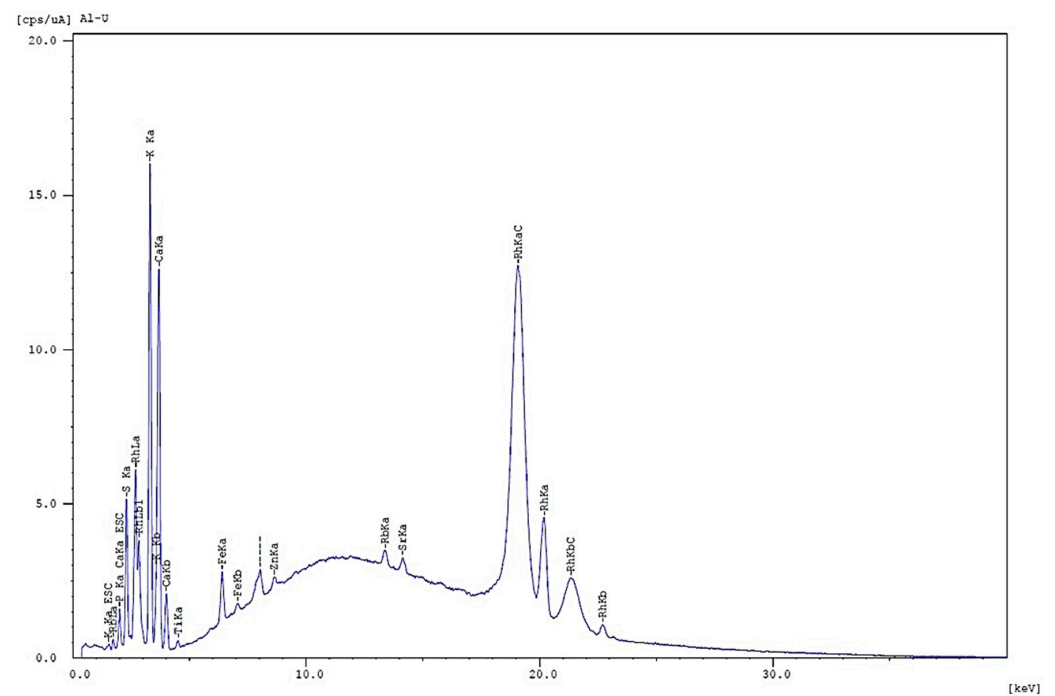

Figure 10. DSC curves of the seed shell of the Neem plant: red line synthetic air atmosphere and black line nitrogen atmosphere.

Table 4. Results of DSC of the Neem seed shell in the atmosphere of synthetic air and nitrogen.

	Synthetic Air			
Event	$T_{onset}/°C$	$T_{peak}/°C$	$T_{endset}/°C$	ΔH, J/g
1	67.1	102.7	142.5	291.5 (endo)
2	244.8	338.1	377.1	7636 (exo)
3	424.0	704.3	723.7	
	Nitrogen			
Event	$T_{onset}/°C$	$T_{peak}/°C$	$T_{endset}/°C$	ΔH, J/g
1	64.5	100.4	143.3	318.6 (endo)
2	250.0	339.1	358.6	554.4 (exo)

Figure 11 and Table 5 show the XRF emission spectrum and elements detected for the Neem seed shell.

Figure 11. X-ray fluorescence spectrum of the seed shell of the Neem plant.

Table 5. X-ray fluorescence analysis: elements detected (%) in the Neem seed shell.

Element	Result	cps/uA
Ca	44.263%	72.2786
K	39.801%	90.9664
S	8.770%	25.1407
P	4.172%	5.7994
Fe	1.806%	13.1290
Ti	0.672%	1.4425
Zn	0.244%	3.8564
Rb	0.156%	6.3434
Sr	0.116%	5.3164

4. Discussion

Neem seed shell showed a moisture content of 12.68% ($\pm$0.16), which is higher than the results found by Fernandes [60] and Santana et al. [61] in their respective studies with the leaves (10.4%) and wood (7.33%) of the Neem. According to Motta et al. [68], in energy applications it is possible to work with a moisture content of around 15%. Quirino et al. [69] presented in their study the moisture contents of various lignocellulosic biomasses between 10.4 and 25.8%. The biomasses of coconut shell [62], sugarcane bagasse [63], and eucalyptus wood [64], used in this work for a comparative purpose, showed moisture contents between 7.32% and 9.03% (see Table 1). Thus, the Neem seed shell showed a moisture content compatible with other biomasses used as fuel. However, it is essential to point out that high moisture reduces the combustibility of the material, and the principal process of using biomass for energy generation is by direct combustion; it is necessary to maintain the moisture content below 25% [42,66,67,70,71].

Regarding the total solid content, the Neem seed shell obtained a value of 87.85 $\pm$ 0.16%, which was applied in the ash content calculation, with the result of 3.80 $\pm$ 0.44%. According to Motta et al. [68] and Quirino et al. [69], which evaluated the leaves and wood of the Neem, ash contents were 7.41% [60] and 0.46% [61], respectively. For the biomasses coconut shell [62], sugarcane bagasse [63], and eucalyptus wood [64], the ash contents reported were 1.44%, 2.15%, and 0.54%, respectively. Like moisture, a high ash content also impacts the Higher Heating Value of biomass [72] and causes ignition and combustion problems [65–67,73]. O ponto de fusão das cinzas dissolvidas pode ser baixo, o que causa problemas de incrustação e escória. The melting point of dissolved ash can be low, which causes incrustation and slag problems. Combustion efficiency is also affected by the ash content, because if combustion does not occur properly, it will require more oxygen for the material to burn completely. Among the combustion technologies available for the use of biomass, fluidized bed combustion is the best suited for burning a low-quality fuel with a high ash content and low HHV [65]. According to ash content, Neem seed shell is suitable for energy use compared to other biomasses reported in the literature.

Regarding volatile matter content, the Neem seed shell presented a value of 81.76 $\pm$ 1.30%. According to data from the literature [Motta et al. [68] and Quirino et al. [69]], the leaves and wood of Neem have values of 92.59% and 82.29% (see Figure 6), respectively. The other biomasses, coconut husk [62], sugarcane bagasse [63], and eucalyptus wood [64], showed results between 69.21% and 86.73%. The volatile matter content is closely related to the energy used in biomass ignition; a high value facilitates the process and the initial stages of combustion [41]. Additionally, too fast an ignition could result in the quick burning of the entire material. The volatile matter content of the Neem seed shell was compatible with biomasses used as fuels [65,69].

For the fixed carbon content, the value 14.44 $\pm$ 1.74% was obtained (see Table 1). As for Neem leaves and wood, Motta et al. [68] and Quirino et al. [69] found values of 24.82% and 17.25% (see Figure 6), respectively. For the coconut shell biomass [62], sugarcane bagasse [63], and eucalyptus wood [64], the values of 30.09%, 15.12%, and 12.73% were reported, respectively. According to Marafon et al. [67], the fixed carbon content is directly proportional to the lignin content, extractives, and biomass density. Thus, a high FC(%) increases the calorific value and, consequently, the production of energy [74,75]. According to the results, Neem seed shell has the potential for use as fuel, compatible with other biomasses reported in the literature [65].

For the Higher Heating Value (HHV), which represents an important parameter to evaluate the energy efficiency of fuels [76], results were obtained for the Neem seed shell in order of 16.949 MJ/kg to 20.404 MJ/kg (see Figure 7), depending on the equation used (see Materials and Methods). HHV refers to the energy released during the complete burning of fuel, assuming that all vapor produced in the combustion is condensed and heat is recovered [70,71,77]. In biomass, HHV varies according to species, moisture content, density, age, and other characteristics [78–82]. The authors used seven equations based on proximate analysis to estimate the HHV of the biomasses. The results for the Neem

shell, leaves, and wood are shown in Figure 7, and those for the coconut shell, sugarcane bagasse, and eucalyptus wood are in Table 2. Among Neem biomasses, leaves showed the highest value. This behavior may be due to differences in organic fractions of the materials; according to Smith et al. [83], Neem leaves have a low carbohydrate content (O-alkyl carbon), a high alkyl-C value, and in FTIR analysis showed pronounced signals at 2920, 2852, 1640, and 1512 cm^{-1}, indicating asymmetric C-H stretches, symmetric C-H stretches, amide I-aromatic ring modes, and aromatic skeletal vibration of lignin, respectively. Comparing the HHV results of reported biomasses, sugarcane bagasse presented an average value of 19.156 MJ/kg. This biofuel is already used in Brazil and applied in cogeneration plants in the sugar and alcohol sector [84]. Furthermore, sugarcane bagasse is a renewable alternative to fossil fuels, contributing to greenhouse gas emissions reduction [85,86]. Coconut shell and eucalyptus wood also showed average values of HHV of 19.864 MJ/kg and 19.422 MJ/kg, respectively. This information represents the importance of biomass for energy purposes and verifies that the HHV of Neem seed shell is within standards already used in the industry.

According to TG-DTG curves of the Neem seed shell (Figures 8 and 9), there are three main degradation events in synthetic air and two in nitrogen. In the oxidative atmosphere, the first event represents the moisture loss (57.8–135.2 °C), the second represents the mass loss attributed to the release of volatile materials (243.2–357.3 °C), and also the decomposition of hemicellulose, cellulose, and partial degradation of lignin [43,45,47,48], and the third event represents the decomposition of cellulose and the lignin (414.3 and 733.6 °C). In the nitrogen atmosphere, the first event represents the moisture loss (54.9–137.2 °C), and the second represents the mass loss attributed to the release of volatile materials and decomposition of hemicellulose, cellulose, and partial degradation of lignin (241.8 and 355.1 °C) [43,87]; see Table 3. According to Yang et al. (2007), the degradation zone of the hemicellulose occurs between 220 and 315 °C, the cellulose between 315 and 400 °C, and the lignin between 160 and 900 °C [88]. For Saikia and Bardalai (2017), the differences in biomass thermograms were due to the variation of proportions of hemicellulose, cellulose, and lignin with traces of minerals and extractives [89], and degradation regions were 220–315 °C for hemicellulose, 315–400 °C for cellulose, and above 450 °C for lignin.

In DSC curves, the first endothermic event was associated with water evaporation (synthetic air 67.1–142.5 °C and nitrogen 64.5–143.3 °C). According to Kozlov et al. (2021), differential scanning calorimetry allows the evaluation of the effect of evaporation on the deviation of the sample temperature from the heating gas temperature [90]. The subsequent events in the oxidative atmosphere can be attributed to the decomposition of hemicellulose, cellulose, and lignin [91]. The energy involved in each event can be seen in Table 4.

X-ray fluorescence is an analytical tool for quantitative elemental analysis of many elements, such ash-formers (e.g., Na, Mg, Al, Si, P, S, K, Ca, Mn, and Fe), and those which can cause adverse effects on the environment (e.g., S, Cl) [49]. Given the increase in the utilization and trade of biomass, the quantitative elemental analysis by XRF is essential information that allows us to evaluate the contaminants, dirt, type, and origin of biomass. The results of the Neem seed shell are shown in Table 5, and the elements with higher percentual were Ca, K, S, and P. According to Vassilev et al. (2010) [92], it is commonly accepted that the concentration and behavior of elements such as Ca, Cl, K, Na, P, S, Si, and heavy metals can cause technological and environmental problems during biomass processing, including combustion. However, studies with other solid fuels indicate that the occurrence of these problems can be connected to the abundance and behavior of modes of element occurrence in biomass and its products [93–95]. Thus, systematic studies about the elements of biomass and their products are in the initial investigation stage and need more assessment for further clarification. The element quantities and order of abundance detected in the Neem seed shell are compatible with other biomasses used as biofuel [92].

5. Conclusions

The moisture content of the Neem seed shell showed values closely established range for biomass used as biofuel, which can be indicated as an option for energy purposes. This parameter also indicates that biomass will present an efficient energy generation. Ash content showed a low value suggesting a characteristic favorable to the increase of HHV. Low moisture and ash contents reinforce that Neem seed shells can present positive results if applied as fuel. The volatile matter and fixed carbon contents also were compatible with other biomass used as fuels. Higher Heating Value showed results closely aligned with sugarcane bagasse, a consolidated biomass already used in energy generation in Brazil, whose capacity in operation corresponds to 70.5% of the total thermoelectric plants, that is, 2440 MW, according to data from the 2030 National Energy Plan of the Ministry of Mines and Energies. The thermograms revealed compatible behaviors with other biomasses presenting the main events attributed to the devolatilization and degradation of hemicellulose, cellulose, and lignin. The degradation of lignocellulosic components involved the highest energy (DSC: oxidative atmosphere). Finally, in XRF analysis, the element quantities and order of abundance detected following the other organic raw materials applied to bioenergy production. All results reinforce the energetic potential of the Neem seed shell and demonstrate yet another application. It is also worth noting that the Neem seed shells can be used in a mixture with other residual biomass for briquette production, further improving its fuel performance.

Author Contributions: Conceptualization, F.S.N., A.L. and M.R.; methodology, F.S.N., M.M.N. and A.S.; software, F.S.N., M.M.N., L.D., B.S. and M.R.; formal analysis, F.S.N., L.D., B.S., S.M., R.M. and M.R.; investigation, F.S.N., M.M.N. and A.S.; resources, F.S.N., M.M.N. and A.S.; data curation, F.S.N., J.S. and M.R.; writing—original draft preparation, F.S.N.; writing—review and editing, M.R. and A.L.; visualization, M.R. and A.L.; supervision, M.R. and A.L.; project administration, M.R. and A.L.; funding acquisition, M.R. and A.L. All authors have read and agreed to the published version of the manuscript.

Data Availability Statement: All data are available in the manuscript.

Conflicts of Interest: The authors declare no conflict of interest.

References

1. Bilal, M.; Iqbal, H.M.N.; Hu, H.; Wang, W.; Zhang, X. Metabolic Engineering and Enzyme-Mediated Processing: A Biotechnological Venture towards Biofuel Production–A Review. *Renew. Sustain. Energy Rev.* **2018**, *82*, 436–447. [CrossRef]
2. Quayson, E.; Amoah, J.; Rachmadona, N.; Hama, S.; Yoshida, A.; Kondo, A.; Ogino, C. Biodiesel-Mediated Biodiesel Production: A Recombinant Fusarium Heterosporum Lipase-Catalyzed Transesterification of Crude Plant Oils. *Fuel Process. Technol.* **2020**, *199*, 106278. [CrossRef]
3. Robles-Medina, A.; González-Moreno, P.A.; Esteban-Cerdán, L.; Molina-Grima, E. Biocatalysis: Towards Ever Greener Biodiesel Production. *Biotechnol. Adv.* **2009**, *27*, 398–408. [CrossRef] [PubMed]
4. Narwal, S.K.; Gupta, R. Biodiesel Production by Transesterification Using Immobilized Lipase. *Biotechnol. Lett.* **2013**, *35*, 479–490. [CrossRef] [PubMed]
5. Eder, L.V.; Provornaya, I.V.; Filimonova, I.V.; Kozhevin, V.D.; Komarova, A.V. World Energy Market in the Conditions of Low Oil Prices, the Role of Renewable Energy Sources. *Energy Proc.* **2018**, *153*, 112–117. [CrossRef]
6. Okoro, O.V.; Sun, Z.; Birch, J. Lipases for Biofuel Production. In *Encyclopedia of Food Chemistry*; Elsevier: Amsterdam, The Netherlands, 2019; pp. 150–157.
7. Narisetty, V.R.R.; Tarafdar, A.; Bachan, N.; Madhavan, A.; Tiwari, A.; Chaturvedi, P.; Varjani, S.; Sirohi, R.; Kumar, V.; Awasthi, M.K.; et al. An Overview of Cellulase Immobilization Strategies for Biofuel Production. *Bioenergy Res.* **2022**, *16*, 4–15. [CrossRef]
8. Hossain, N.; Bhuiyan, M.A.; Pramanik, B.K.; Nizamuddin, S.; Griffin, G. Waste Materials for Wastewater Treatment and Waste Adsorbents for Biofuel and Cement Supplement Applications: A Critical Review. *J. Clean Prod.* **2020**, *255*, 120261. [CrossRef]
9. Beltrami, F.; Fontini, F.; Grossi, L. The Value of Carbon Emission Reduction Induced by Renewable Energy Sources in the Italian Power Market. *Ecol. Econ.* **2021**, *189*, 107149. [CrossRef]

10. Chu, R.; Li, S.; Zhu, L.; Yin, Z.; Hu, D.; Liu, C.; Mo, F. A Review on Co-Cultivation of Microalgae with Filamentous Fungi: Efficient Harvesting, Wastewater Treatment and Biofuel Production. *Renew. Sustain. Energy Rev.* **2021**, *139*, 110689. [CrossRef]

11. Hussain, F.; Shah, S.Z.; Ahmad, H.; Abubshait, S.A.; Abubshait, H.A.; Laref, A.; Manikandan, A.; Kusuma, H.S.; Iqbal, M. Microalgae an Ecofriendly and Sustainable Wastewater Treatment Option: Biomass Application in Biofuel and Bio-Fertilizer Production. A Review. *Renew. Sustain. Energy Rev.* **2021**, *137*, 110603. [CrossRef]

12. Merlin, A.Z.; Marcel, O.A.; Louis Max, A.O.; Salem, C.; Jean, G. Development and Experimental Investigation of a Biodiesel from a Nonedible Woody Plant: The Neem. *Renew. Sustain. Energy Rev.* **2015**, *52*, 201–208. [CrossRef]

13. Rajaseenivasan, T.; Srinivasan, V.; Syed Mohamed Qadir, G.; Srithar, K. An Investigation on the Performance of Sawdust Briquette Blending with Neem Powder. *Alex. Eng. J.* **2016**, *55*, 2833–2838. [CrossRef]

14. Takase, M.; Zhao, T.; Zhang, M.; Chen, Y.; Liu, H.; Yang, L.; Wu, X. An Expatiate Review of Neem, Jatropha, Rubber and Karanja as Multipurpose Non-Edible Biodiesel Resources and Comparison of Their Fuel, Engine and Emission Properties. *Renew. Sustain. Energy Rev.* **2015**, *43*, 495–520. [CrossRef]

15. Venzon, M.; Togni, P.H.B.; Perez, A.L.; Oliveira, J.M. Control of Two-Spotted Spider Mites with Neem-Based Products on a Leafy Vegetable. *Crop. Prot.* **2020**, *128*, 105006. [CrossRef]

16. Abbah, E.C.; Nwandikom, G.I.; Egwuonwu, C.C.; Nwakuba, N.R. Effect of Reaction Temperature on the Yield of Biodiesel from Neem Seed Oil. *Am. J. Energy Sci.* **2016**, *3*, 16–20.

17. Parckert, E.E.D.T.; Finzer, J.R.D. Extração de óleo de Nim por prensagem mecânica. Anais do Congresso Brasileiro de Engenharia Química. Volume 1. 2016. Available online: https://proceedings.science/cobeq/cobeq-2016/trabalhos/extracao-de-oleo-de-nim-por-prensagem-mecanica?lang=pt-br (accessed on 8 April 2023).

18. Paes, J.B.; Souza, A.D.D.; Lima, C.R. De Rendimento e Características Físicas Dos Óleos de Nim (*Azadirachta Indica*) e Mamona (*Ricinus Communis*). *Floresta E Ambiente* **2016**, *22*, 134–139. [CrossRef]

19. Chatterjee, S.; Bag, S.; Biswal, D.; Sarkar Paria, D.; Bandyopadhyay, R.; Sarkar, B.; Mandal, A.; Dangar, T.K. Neem-Based Products as Potential Eco-Friendly Mosquito Control Agents over Conventional Eco-Toxic Chemical Pesticides–A Review. *Acta Trop.* **2023**, *240*, 106858. [CrossRef]

20. Benelli, G. Plant-Mediated Synthesis of Nanoparticles: A Newer and Safer Tool against Mosquito-Borne Diseases? *Asian Pac. J. Trop. Biomed.* **2016**, *6*, 353–354. [CrossRef]

21. Benelli, G. Research in Mosquito Control: Current Challenges for a Brighter Future. *Parasitol. Res.* **2015**, *114*, 2801–2805. [CrossRef]

22. Benelli, G.; Bedini, S.; Cosci, F.; Toniolo, C.; Conti, B.; Nicoletti, M. Larvicidal and Ovideterrent Properties of Neem Oil and Fractions against the Filariasis Vector Aedes Albopictus (Diptera: *Culicidae*): A Bioactivity Survey across Production Sites. *Parasitol. Res.* **2015**, *114*, 227–236. [CrossRef]

23. Benelli, G.; Canale, A.; Toniolo, C.; Higuchi, A.; Murugan, K.; Pavela, R.; Nicoletti, M. Neem (*Azadirachta Indica*): Towards the Ideal Insecticide? *Nat. Prod. Res.* **2017**, *31*, 369–386. [CrossRef]

24. Saleem, S.; Muhammad, G.; Hussain, M.A.; Bukhari, S.N.A. A Comprehensive Review of Phytochemical Profile, Bioactives for Pharmaceuticals, and Pharmacological Attributes of *Azadirachta Indica*. *Phytother. Res.* **2018**, *32*, 1241–1272. [CrossRef]

25. Dua, V.K.; Pandey, A.C.; Raghavendra, K.; Gupta, A.; Sharma, T.; Dash, A.P. Larvicidal Activity of Neem Oil (*Azadirachta Indica*) Formulation against Mosquitoes. *Malar. J.* **2009**, *8*, 124. [CrossRef] [PubMed]

26. Wan, M.T.; Watts, R.G.; Isman, M.B.; Strub, R. Evaluation of the Acute Toxicity to Juvenile Pacific Northwest Salmon of Azadirachtin, Neem Extract, and Neem-Based Products. *Bull. Environ. Contam. Toxicol.* **1996**, *56*, 432–439. [CrossRef] [PubMed]

27. Jacobson, M. *Focus on Photochemicals Pesticides*; Volume I: The Neem Tree; Jacobson, M., Ed.; CRC Press, Inc.: Boca Raton, MI, USA, 1988.

28. Anjali, C.; Sharma, Y.; Mukherjee, A.; Chandrasekaran, N. Neem Oil (*Azadirachta Indica*) Nanoemulsion–A Potent Larvicidal Agent against Culex Quinquefasciatus. *Pest. Manag. Sci.* **2012**, *68*, 158–163. [CrossRef] [PubMed]

29. Roy, P.; Das, B.; Mohanty, A.; Mohapatra, S. Green Synthesis of Silver Nanoparticles Using Azadirachta Indica Leaf Extract and Its Antimicrobial Study. *Appl. Nanosci.* **2017**, *7*, 843–850. [CrossRef]

30. Iqbal, N.; Agrawal, A.; Kumar, J. Development of Effervescent Tablet Formulation for Rapid Control of Mosquito Problem in Early Stages from Different Breeding Sites. *Arab. J. Chem.* **2021**, *14*, 103082. [CrossRef]

31. Bhaskara Rao, T.S.S.; Murugan, S. Experimental Investigation of Drying Neem (*Azadirachta Indica*) in an Evacuated Tube Solar Dryer: Performance, Drying Kinetics and Characterization. *Sol. Energy* **2023**, *253*, 270–284. [CrossRef]

32. Singh, P.; Vyas, S.; Yadav, A. Experimental Comparison of Open Sun Drying and Solar Drying Based on Evacuated Tube Collector. *Int. J. Sustain. Energy* **2019**, *38*, 348–367. [CrossRef]

33. Subapriya, R.; Nagini, S. Medicinal Properties of Neem Leaves: A Review. *Curr. Med. Chem. Anti Cancer Agents* **2005**, *5*, 149–156. [CrossRef]

34. Kumar, S.; MuthuDineshkumar, R.; Angkayarkan Vinayakaselvi, M.; Ramanathan, A. Enhancing Environmental Sustainability through Waste to Energy Conversion of Neem Leaves. *Mater. Today Proc.* **2021**, *46*, 10060–10064. [CrossRef]

35. Espuelas, S.; Marcelino, S.; Echeverría, A.M.; del Castillo, J.M.; Seco, A. Low Energy Spent Coffee Grounds Briquetting with Organic Binders for Biomass Fuel Manufacturing. *Fuel* **2020**, *278*, 118310. [CrossRef]

36. Han, K.; Gao, J.; Qi, J. The Study of Sulphur Retention Characteristics of Biomass Briquettes during Combustion. *Energy* **2019**, *186*, 115788. [CrossRef]

37. Wang, D.; Liu, L.; Yuan, Y.; Yang, H.; Zhou, Y.; Duan, R. Design and Key Heating Power Parameters of a Newly-Developed Household Biomass Briquette Heating Boiler. *Renew. Energy* **2020**, *147*, 1371–1379. [CrossRef]
38. Guo, Z.; Wu, J.; Zhang, Y.; Wang, F.; Guo, Y.; Chen, K.; Liu, H. Characteristics of Biomass Charcoal Briquettes and Pollutant Emission Reduction for Sulfur and Nitrogen during Combustion. *Fuel* **2020**, *272*, 117632. [CrossRef]
39. Nagarajan, J.; Prakash, L. Preparation and Characterization of Biomass Briquettes Using Sugarcane Bagasse, Corncob and Rice Husk. *Mater. Today Proc.* **2021**, *47*, 4194–4198. [CrossRef]
40. Adeleke, A.A.; Odusote, J.K.; Ikubanni, P.P.; Agboola, O.O.; Balogun, A.O.; Lasode, O.A. Tumbling Strength and Reactivity Characteristics of Hybrid Fuel Briquette of Coal and Biomass Wastes Blends. *Alex. Eng. J.* **2021**, *60*, 4619–4625. [CrossRef]
41. Braz, C.E.M. Caracterização de Biomassa Lignocelulósica para uso em Processos Térmicos de Geração de Energia. Master's Thesis, Universidade Estadual Paulista, São Paulo, Brazil, 2014.
42. Carvalho, N.; Barros, J.; Silva, D.; Nakashima, G.; Yamaji, F. Caracterização Física e Química da Biomassa Usada Como Combustível Sólido em Uma Caldeira. *Quim Nova* **2020**, *44*, 35–40. [CrossRef]
43. Carvalho, P.R.; Medeiros, S.L.S.; Paixão, R.L.; Figueredo, I.M.; Mattos, A.L.A.; Rios, M.A.S. Thermogravimetric Pyrolysis of Residual Biomasses Obtained Post-Extraction of Carnauba Wax: Determination of Kinetic Parameters Using Friedman's Isoconversional Method. *Renew Energy* **2023**, *207*, 703–713. [CrossRef]
44. Silva, C.; Sousa, B.; Nunes, J.; Malveira, J.; Marques, R.; Damasceno, L.; Braga, E.; Lessa, T.; Bertini, L.; Maciel, M.; et al. Evaluation of Babassu Cake Generated in the Extraction of the Oil as Feedstock for Biofuel Production. *Processes* **2023**, *11*, 585. [CrossRef]
45. de Luna, Y.M.; Marcelo Rodrigues, P.; Antônia Mabrysa Torres, G.; Antônio Eufrázio, d.C.J.; Jackson Queiroz, M.; Selma Elaine, M.; de Sousa, M.A.R. A Thermogravimetric Analysis of Biomass Wastes from the Northeast Region of Brazil as Fuels for Energy Recovery. *Energy Sources Part A Recovery Util. Environ. Eff.* **2019**, *41*, 1557–1572. [CrossRef]
46. Torres Gadelha, A.M.; Lima Almeida, F.D.; Silva, R.A.; Malveira, J.Q.; Sanders Lopes, A.A.; De Sousa Rios, M.A. Cashew Nut Husk and Babassu Coconut Husk Residues: Evaluation of Their Energetic Properties. *Energy Sources Part A Recovery Util. Environ. Eff.* **2018**, *5*, 2146–2156. [CrossRef]
47. Saikia, N.; Bardalai, M. Thermal Analysis and Kinetic Parameters Determination of Biomass Using Differential Thermal Gravimetric Analysis in N_2 Atmosphere. *Mater. Today Proc.* **2018**, *5*, 2146–2156. [CrossRef]
48. Gill, P.; Moghadam, T.T.; Ranjbar, B. Differential Scanning Calorimetry Techniques: Applications in Biology and Nanoscience. *J. Biomol. Tech.* **2010**, *21*, 167–193. [PubMed]
49. Morgan, T.J.; George, A.; Boulamanti, A.K.; Álvarez, P.; Adanouj, I.; Dean, C.; Vassilev, S.V.; Baxter, D.; Andersen, L.K. Quantitative X-ray Fluorescence Analysis of Biomass (Switchgrass, Corn Stover, Eucalyptus, Beech, and Pine Wood) with a Typical Commercial Multi-Element Method on a WD-XRF Spectrometer. *Energy Fuels* **2015**, *29*, 1669–1685. [CrossRef]
50. Araújo, D.M. *Estudo do Comportamento da Co-Combustão da Borra de Café e do Bagaço de Cana-de-Açúcar*; Universidade Federal da Paraíba: João Pessoa, Brazil, 2021.
51. *ABNT NBR 16550*; Bagaço de Cana–Caracterização Química. ABNT: Brasília, Brazil, 2018.
52. *ASTM D3175-20*; ASTM International Standard Test Method for Volatile Matter in the Analysis Sample of Coal and Coke. ASTM: West Conshohocken, PA, USA, 2020; pp. 1–14.
53. *ASTM D3172-89*; ASTM International Standard Practice for Proximate Analysis of Coal and Coke. ASTM: West Conshohocken, PA, USA, 2021; pp. 1–2.
54. Parikh, J.; Channiwala, S.A.; Ghosal, G.K. A Correlation for Calculating HHV from Proximate Analysis of Solid Fuels. *Fuel* **2005**, *84*, 487–494. [CrossRef]
55. Özyuğuran, A.; Yaman, S. Prediction of Calorific Value of Biomass from Proximate Analysis. *Energy Procedia* **2017**, *107*, 130–136. [CrossRef]
56. Callejón-Ferre, A.J.; Velázquez-Martí, B.; López-Martínez, J.A.; Manzano-Agugliaro, F. Greenhouse Crop Residues: Energy Potential and Models for the Prediction of Their Higher Heating Value. *Renew. Sustain. Energy Rev.* **2011**, *15*, 948–955. [CrossRef]
57. Yin, C.-Y. Prediction of Higher Heating Values of Biomass from Proximate and Ultimate Analyses. *Fuel* **2011**, *90*, 1128–1132. [CrossRef]
58. Demirbaş, A. Calculation of Higher Heating Values of Biomass Fuels. *Fuel* **1997**, *76*, 431–434. [CrossRef]
59. Phichai, K.; Pragrobpondee, P.; Khumpart, T.; Hirunpraditkoon, S. Prediction Heating Values of Lignocellulosics from Biomass Characteristics. *Int. J. Chem. Mol. Eng.* **2013**, *7*, 532–535. [CrossRef]
60. Fernandes, L.A.A. *Reuse of Waste from Azadirachta Indica Pruning for the Production of Briquettes*; Federal University of Campina Grande: Campina Grande, Brazil, 2018; pp. 1–37.
61. Santana, R.N. Energy Characterization of Charcoal from Azadirachta Indica Juss (Neem), South of Tocantins. In Proceedings of the International Biomass Congress, Nashville, TN, USA, 3–5 February 2020; pp. 1–7.
62. Alves, M.B.F.; Candeia, R.A.; Leite, J.C.A.; Dos Santos, A.F. Produção e Caracterização de Biocombustível Sólido a Partir de Resíduos Orgânicos Sem Tratamento Térmico/Production and Characterization of Solid Biofuel from Organic Waste without Thermal Treatment. *Braz. J. Dev.* **2022**, *8*, 8925–8945. [CrossRef]
63. Costa, L.A.A.C.; Eufrade, H., Jr.; Spadim, E.R.; Da Silva, J.M.S.; Guerra, S.P.S. Caracterização Física, Química e Mêcanica de Pellets de Bagaço de Cana-de-Açúcar. *Energ. Na Agric.* **2020**, *35*, 38–45. [CrossRef]

64. Barbosa, B.M.; Siqueira, H.F.; Cabral, C.P.T.; Cândido, W.L.; Silva, C.M.S.; de Carneiro, A.C.O.; Aguiar, A.R. Qualidade de Briquetes Produzidos a Partir do Mix de Resíduo Agroindustrial com Eucalipto. In *Recursos Naturais: Energia de Biomassa Florestal*; Editora Científica Digital: São Paulo, Brazil, 2021; pp. 185–196.

65. Saidur, R.; Abdelaziz, E.A.; Demirbas, A.; Hossain, M.S.; Mekhala, S. A Review on Biomass as a Fuel for Boilers. *Renew. Sustain. Energy Rev.* **2011**, *15*, 2262–2289. [CrossRef]

66. da Silva, D.A. Interdependência Linear do Poder Calorífico Superior em Função da Análise Imediata em Materiais Ligno-celulósicos. Master's Thesis, Universidade Federal de São Carlos, São Carlos, Brazil, 2019.

67. Marafon, A.C.; Santiago, A.D.; Amaral, A.F.C.; Bierhals, A.N.; Paiva, H.L.; Guimaraes, V.S. Uso da Biomassa Para a Geração de Energia–Portal Embrapa. Available online: https://www.embrapa.br/en/busca-de-publicacoes/-/publicacao/1063559/uso-da-biomassa-para-a-geracao-de-energia (accessed on 8 April 2023).

68. Motta, I.L.; Miranda, N.T.; Maciel Filho, R.; Wolf Maciel, M.R. Biomass Gasification in Fluidized Beds: A Review of Biomass Moisture Content and Operating Pressure Effects. *Renew. Sustain. Energy Rev.* **2018**, *94*, 998–1023. [CrossRef]

69. Quirino, W.F.; Vale, A.D.; Andrade, A.D.; Abreu, V.L.S.; Azevedo, A.D.S. Poder Calorífico da Madeira e de Materiais Ligno-Celulósicos. *Rev. Madeira* **2005**, *89*, 100–106.

70. Siebeneichler, E.A.; Costa, L.M.d.; Figueredo, N.A.; Tronto, J.; Rocha, P.A. Influência de Temperatura e Taxas de Aquecimento Na Resistência Mecânica, Densidade e Rendimento do Carvão da Madeira de Eucalyptus Cloeziana. *Rev. Ciência Madeira RCM* **2017**, *8*, 82–94. [CrossRef]

71. Neiva, P.S.; Furtado, D.B.; Finzer, J.R.D. Capacidade Térmica E Poder Calorífico De Biomassa Eucalipto. II Encontro de Desenvolvimento de Processos Agroindustriais, Uniube. 2018. Available online: https://repositorio.uniube.br/bitstream/123456789/922/1/CAPACIDADE%20T%C3%89RMICA%20E%20PODER%20CALORIFICO%20DE%20BIOMASSA%20EUCALIPTO.pdf (accessed on 8 April 2023).

72. Souza, L.M.d.; Bezerra, J.B.; de Queiroz, W.L.V.; Trugilho, P.F.; Protásio, T.D.P.; de Souza, T.M.; Bufalino, L. Comparação da Qualidade dos Tecidos do Pecíolo de Buriti (*Mauritia Flexuosa* L.f.) Para Combustão e Carbonização. *Ciência Florest.* **2020**, *30*, 516. [CrossRef]

73. de Protásio, P.T.; Scatolino, M.V.; de Araújo, A.C.C.; de Oliveira, A.F.C.F.; de Figueiredo, I.C.R.; de Assis, M.R.; Trugilho, P.F. Assessing Proximate Composition, Extractive Concentration, and Lignin Quality to Determine Appropriate Parameters for Selection of Superior Eucalyptus Firewood. *Bioenergy Res.* **2019**, *12*, 626–641. [CrossRef]

74. Motghare, K.A.; Rathod, A.P.; Wasewar, K.L.; Labhsetwar, N.K. Comparative Study of Different Waste Biomass for Energy Application. *Waste Manag.* **2016**, *47*, 40–45. [CrossRef]

75. Nones, D.L.; Brand, M.A.; Da Cunha, A.B.; De Carvalho, A.F.; Weise, S.M.K. Determinação das Propriedades Energéticas da Madeira e do Carvão Vegetal Produzido A Partir de Eucalyptus Benthamii. *Floresta* **2014**, *45*, 57. [CrossRef]

76. Lunguleasa, A.; Spirchez, C.; Zeleniuc, O.; Lunguleasa, A.; Spirchez, C.; Zeleniuc, O. Evaluation of the Calorific Values of Wastes from Some Tropical Wood Species. *Maderas. Cienc. Y Tecnol.* **2020**, *22*, 269–280. [CrossRef]

77. Bhalerao, M.; Pangavhane, P.; Dhamangaonkar, P. Development of a Correlation for the Estimation of the Higher Calorific Value of Diesel, Based on Its Kinematic Viscosity and Density. *Adv. Sci. Eng. Med.* **2021**, *12*, 1040–1043. [CrossRef]

78. Pawar, S.; Hole, J.; Bankar, M.; Khan, S.; Wankhade, S. Use of Fatty Acid Chemical Composition for Predicting Higher Calorific Value of Biodiesel. *Mater. Today Proc.* **2023**. [CrossRef]

79. Vallejo, F.; Díaz-Robles, L.A.; Vega, R.; Cubillos, F. A Novel Approach for Prediction of Mass Yield and Higher Calorific Value of Hydrothermal Carbonization by a Robust Multilinear Model and Regression Trees. *J. Energy Inst.* **2020**, *93*, 1755–1762. [CrossRef]

80. Debdoubi, A.; El Amarti, A.; Colacio, E. Production of Fuel Briquettes from Esparto Partially Pyrolyzed. *Energy Convers. Manag.* **2005**, *46*, 1877–1884. [CrossRef]

81. Kumar, J.A.; Kumar, K.V.; Petchimuthu, M.; Iyahraja, S.; Kumar, D.V. Comparative Analysis of Briquettes Obtained from Biomass and Charcoal. *Mater. Today Proc.* **2021**, *45*, 857–861. [CrossRef]

82. Jowkar, A.; Sereshki, F.; Najafi, M. Numerical Simulation of UCG Process with the Aim of Increasing Calorific Value of Syngas. *Int. J. Coal. Sci. Technol.* **2020**, *7*, 196–207. [CrossRef]

83. Smith, B.A.M.; Eudoxie, G.; Stein, R.; Ramnarine, R.; Raghavan, V. Effect of Neem Leaf Inclusion Rates on Compost Physico-Chemical, Thermal and Spectroscopic Stability. *Waste Manag.* **2020**, *114*, 136–147. [CrossRef]

84. Ponte, M.R.; Gadelha, A.M.T.; Machado, Y.L.; Lopes, A.A.S.; Malveira, J.Q.; Mazzetto, S.E.; Lomonaco, D.; de Sousa Rios, M.A. Blendas de Bagaço de Cana-de-Açúcar, Podas de Mangueira e Cajueiro: Caracterização das Propriedades e Investigação de Seus Potenciais Energéticos. *Matéria* **2019**, *24*, e12372. [CrossRef]

85. Wu, N.; Ji, T.; Huang, P.; Fu, T.; Zheng, X.; Xu, Q. Use of Sugar Cane Bagasse Ash in Ultra-High Performance Concrete (UHPC) as Cement Replacement. *Constr. Build. Mater.* **2022**, *317*, 125881. [CrossRef]

86. El Naga, A.O.; El Saied, M.; Shaban, S.A.; El Kady, F.Y. Fast Removal of Diclofenac Sodium from Aqueous Solution Using Sugar Cane Bagasse-Derived Activated Carbon. *J. Mol. Liq.* **2019**, *285*, 9–19. [CrossRef]

87. Dhanavath, K.N.; Bankupalli, S.; Sugali, C.S.; Perupogu, V.; Nandury, V.S.; Bhargava, S.; Parthasarathy, R. Optimization of Process Parameters for Slow Pyrolysis of Neem Press Seed Cake for Liquid and Char Production. *J. Environ. Chem. Eng.* **2019**, *7*, 102905. [CrossRef]

88. Yang, H.; Yan, R.; Chen, H.; Lee, D.H.; Zheng, C. Characteristics of Hemicellulose, Cellulose and Lignin Pyrolysis. *Fuel* **2007**, *86*, 1781–1788. [CrossRef]

89. Liu, L.; Pang, Y.; Lv, D.; Wang, K.; Wang, Y. Thermal and kinetic analyzing of pyrolysis and combustion of self-heating biomass particles. *Process Saf. Environ. Prot.* **2021**, *151*, 39–50. [CrossRef]

90. Kozlov, A.N.; Shamansky, V.A.; Donskoy, I.G.; Penzik, M.V.; Keiko, A.V. A DSC Signal for Studying Kinetics of Moisture Evaporation from Lignocellulosic Fuels. *Thermochim. Acta* **2021**, *698*, 178887. [CrossRef]

91. Candelier, K.; Dibdiakova, J.; Volle, G.; Rousset, P. Study on Chemical Oxidation of Heat Treated Lignocellulosic Biomass under Oxygen Exposure by STA-DSC-FTIR Analysis. *Thermochim. Acta* **2016**, *644*, 33–42. [CrossRef]

92. Vassilev, S.V.; Baxter, D.; Andersen, L.K.; Vassileva, C.G. An Overview of the Chemical Composition of Biomass. *Fuel* **2010**, *89*, 913–933. [CrossRef]

93. Vassilev, S.V.; Vassileva, C.G.; Baxter, D.; Andersen, L.K. A New Approach for the Combined Chemical and Mineral Classification of the Inorganic Matter in Coal. 2. Potential Applications of the Classification Systems. *Fuel* **2009**, *88*, 246–254. [CrossRef]

94. Vassilev, S.V.; Braekman-Danheux, C.; Laurent, P.; Thiemann, T.; Fontana, A. Behaviour, Capture and Inertization of Some Trace Elements during Combustion of Refuse-Derived Char from Municipal Solid Waste. *Fuel* **1999**, *78*, 1131–1145. [CrossRef]

95. Vassilev, S.V.; Vassileva, C.G. Geochemistry of Coals, Coal Ashes and Combustion Wastes from Coal-Fired Power Stations. *Fuel Process. Technol.* **1997**, *51*, 19–45. [CrossRef]